

Nanoscale

Accepted Manuscript



This is an *Accepted Manuscript*, which has been through the Royal Society of Chemistry peer review process and has been accepted for publication.

Accepted Manuscripts are published online shortly after acceptance, before technical editing, formatting and proof reading. Using this free service, authors can make their results available to the community, in citable form, before we publish the edited article. We will replace this *Accepted Manuscript* with the edited and formatted *Advance Article* as soon as it is available.

You can find more information about *Accepted Manuscripts* in the [Information for Authors](#).

Please note that technical editing may introduce minor changes to the text and/or graphics, which may alter content. The journal's standard [Terms & Conditions](#) and the [Ethical guidelines](#) still apply. In no event shall the Royal Society of Chemistry be held responsible for any errors or omissions in this *Accepted Manuscript* or any consequences arising from the use of any information it contains.

Germanium Nanoparticles Encapsulated in Flexible Carbon Nanofibers as Self-Supported Electrodes for High performance Lithium-ion Batteries

*Weihan Li, Zhenzhong Yang, Jianxiu Cheng, Xiongwu Zhong, Lin Gu, Yan Yu**

Abstract

Germanium is a promising high-capacity anode material for lithium ion batteries, but still suffers from poor cyclability due to its huge volume variation during the Li-Ge alloy/dealloy processes. Here we rationally designed a flexible and self-supported electrode consisting of Ge nanoparticles encapsulated in carbon nanofibers (Ge-CNFs) by facile electrospinning technique as potential anodes for Li-ion batteries. The Ge-CNFs exhibits excellent electrochemical performance with a reversible specific capacity of $\sim 1420 \text{ mAhg}^{-1}$ after 100 cycles at 0.15C with only 0.1% decay per cycle (the theoretical specific capacity of Ge is 1624 mAhg^{-1}). When cycled at a high current of 1C, it still delivers a reversible specific capacity of 829 mAhg^{-1} after 250 cycles. The strategy and design is simple, effective, and versatility. This type of flexible electrodes is a promising solution for the development of flexible lithium-ion batteries with high power and energy densities.

Rechargeable lithium-ion batteries (LIBs) have become essential electrochemical energy storage devices for portable electronic devices, such as cell phones, laptop, and digital cameras, and also have been considered as the power source for hybrid electric vehicles (HEV).^[1, 2] To meet the increasing requirements of LIBs with both high energy density and high power density, it is crucial to develop new alternative electrode materials with higher reversible capacity than commercial ones.^[3-10]

W. Li, J. Cheng, X. Zhong, Prof. Y. Yu
CAS Key Laboratory of Materials for Energy Conversion, Department of Materials Science and Engineering,
University of Science and Technology of China, Anhui Hefei 230026, P. R. China
E-mail: yanyumse@ustc.edu.cn
Z. Yang, Prof. L. Gu
Beijing National Laboratory for Condensed Matter Physics, The Institute of Physics, Chinese Academy of
Sciences, Beijing 100190, P. R. China

Compared with the graphite anode (theoretical capacity: 372 mAhg^{-1}), Ge anode for LIBs have received much attention due to its high theoretical capacity (1624 mAhg^{-1} , corresponding to $\text{Li}_{4.4}\text{Ge}$), excellent lithium-ion diffusion coefficient (400 times higher than Si) and high electrical conductivity.^[11-20] However, the practical application of Ge as an anode material is prevented by its poor cyclability. The main reason for the poor capacity retention is attributed to the drastic volume changes during Li-Ge alloying/dealloying process, resulting in both mechanical failure and loss of electrical contact at the current collector.^[8, 19] Another reason is that the formation of Ge nanoparticle aggregation during the discharging process.^[21-23] To minimize such volume strain and enhance the cycling stability of Ge anodes, approaches for versatile morphology control using 0D nanoparticles, 1D nanowires, 1D nanotube, and 3D porous particles have been reported.^[11, 12, 15, 20, 24-29] Among these strategies, 0D Ge nanoparticles encapsulated in carbonaceous materials have been reported to be promising in improving the cycle performance.^[14, 19, 31-33] It has been demonstrated that decreasing the size of Ge particles to the nanoscale can mitigate the mechanical strains and volume change during alloying/dealloying process, resulting in less cracking and particle pulverization.^[31, 32] Moreover, as a buffer of Ge particles volume changes, carbonaceous materials could minimize the mechanical stress to overcome the pulverization and provide both Li^+ and e^- transport paths simultaneously.^[14, 32] Previous studies also show that designing 1D nanostructured such as nanowires, nanofibers, nanorod and nanotubes are quite attractive for electrode materials due to their advantages (large surface to volume ratio, high electrode-electrolyte contact area, fast Li^+ diffusion and good strain accommodation in the open and loose structure), which is superior to that of bulk materials.^[19, 34, 35] However, owing to the complex preparation process of germanium nanoparticles ($< 10 \text{ nm}$), it is still a challenge to get highly dispersed nanoparticles encapsulated in carbon nanofibers.^[32, 36]

Our approach is to synthesize 0D Ge nanoparticles encapsulated in 1D carbon nanofibers (denoted as $(\text{Ge})_{0\text{D}}@(\text{CNFs})_{1\text{D}}$), and form 3D flexible porous Ge-CNFs hybrid films as self-supported electrodes for LIBs. This Ge-CNFs electrode displays

excellent electrochemical performance including little capacity fading over 100 cycles ($\sim 1420 \text{ mAhg}^{-1}$ at 0.15 C after 100 cycles) and good rate capability ($\sim 480 \text{ mAhg}^{-1}$ at 15 C), where the capacity refers to the capacity contribution of Ge. And Even cycled at a current density of 1C, it still delivers a reversible capacity of $\sim 829 \text{ mAhg}^{-1}$ based on the content of Ge after 250 cycles. The superior electrochemical performance of Ge-CNFs electrode can be attributed to the synergistic effects of 0D Ge, 1D CNFs, and 3D interconnected CNFs network. First, this design will provide a variety of advantages: large bare surface accessible by electrolyte, short diffusion length of Li^+/e^- in Ge and high conductivity transport of electrons along the percolating fibers.^[37-39] Second, the 3D interconnected CNFs network could effective buffer the huge volume change during cycling.^[14, 19, 31-33] Furthermore, this self-supported electrode design will simplify the cell packing process by eliminating inactive ingredients such as binders and current collectors, resulting further improvement of both energy density and power density for LIBs.^[40-42]

In this work, Ge nanoparticles encapsulated in 3D interconnected CNFs were prepared by pyrolysis of electrospun 1D nanofibers as flexible free-standing working electrodes for LIBs.^[37, 39, 43, 44] The loading amount of electroactive material (Ge) could be adjusted by simply tuning the weight ratio between tetramethoxygermane (TMOG) and polyacrylonitrile (PAN) in the precursor solution. Fig.1 schematically illustrates the experimental procedures. The precursor solution of TMOG and PAN was electrospun into fibers (Fig. 1A). During the electrospinning process, TMOG in the electrospun polymer fibers reacted with the H_2O in the air to form GeO_2 (Fig. 1B).^[45] The as-spun fibers were then stabilized in air at 280 °C. Afterward, the stabilized fibers were thermally treated in in Ar/H_2 atmosphere at 650 °C. During the carbonization process, PAN was carbonized and GeO_2 particles generated from TMOG was reduced to Ge particles.^[20, 45-47] The obtained Ge-CNFs film was then directly cut and tested as self-supported working eletrodes for LIBs (Fig. 1C&D).

Fig. 2A&2B show the scanning electron microscopy (SEM) images of the as-spun PAN-TMOG fibers and Ge-CNFs, respectively. The as-spun 1D fibers show

a uniform diameter of ~230 nm with a smooth surface. After the two-step thermal treatment, the carbonized fibers maintain the fibrous morphology with no obvious change in diameter and the interconnected network is kept perfectly comparing to the as-electrospun fibers. And the maintained continuous and interconnected structure made of 1D nanofibers can facilitate both electron and Li-ion transfer^[48] and electrolyte access to active materials. As the smooth surface of the fibers suggested, all Ge nanoparticles were encapsulated in the CNFs, avoiding direct exposure of the Ge particles to the electrolyte. And there is no obvious difference between the morphology of CNFs derived from electrospun pure PAN nanofibers (see supporting information, Fig. S5A) and the Ge-CNFs, except for tiny difference of the diameter between the CNFs and Ge-CNFs resulted from instability during the electrospinning.

Transmission electron microscopy (TEM) (Fig. 2C&2D) was further used to investigate the encapsulation of Ge nanoparticles in the CNFs. As shown in the Fig. 2C, the Ge nanoparticles, with particle sizes ranging from 20 nm to 80 nm, were well dispersed inside the carbon fibers. A high-resolution transmission electron microscopy (HRTEM) micrograph, shown in Fig. 2D, displays the fine microstructure of Ge nanoparticles entirely confined in the core of the carbon fiber. The content of Ge in Ge-CNFs was determined by thermogravimetric analysis (TGA) and was calculated to be about 48.1 wt% (see supporting information, Fig. S1).

X-ray diffraction (XRD) and Fourier transform infrared (FTIR) spectroscopy were used to characterize the Ge-CNFs and the as-spun fibers (see supporting information, Fig. S2). As-spun fibers (Fig. S2A) show two broad peaks at around 17° and 28°, corresponding to a hexagonal lattice of PAN, while the stabilized fibers show only wide peak at around 28°. The loss of the broad peak at ~17° is related to changes of the structure of PAN after the first-step thermal treatment.^[49] And the result reveals amorphous phase of fibers before carbonization at high temperature. After carbonization process, four sharp peaks at 27.38, 45.38, 53.78, and 66.08 can be indexed to (111), (220), (311), and (331) reflection of standard cubic phase Ge (JCPDS card No. 4-545). No obvious peaks corresponding to carbon are found in the XRD pattern, indicating that the carbon is amorphous. This result is consistent with

the FTIR spectroscopy (Fig. S2B). With the existence of two bands of C-O and C=C vibration of polymer,^[50] the stabilized fibers shows two typical bands of GeO₂ at 882 cm⁻¹ and 3340 cm⁻¹, which is in accordance with the result of commercial GeO₂.^[47] After reduction process, no GeO₂ peaks were detected in the Ge-CNFs, indicating that the GeO₂ particles were fully reduced to Ge nanoparticles.^[20]

Fig. 3A shows the cyclic voltammograms (CV) curves of Ge-CNFs electrode. Two peaks at 0.02 V and 0.6 V were observed during the first lithiation step, which attribute to lithium alloying with Ge forming Li_xGe alloys and the decomposition of the electrolyte to form the solid-electrolyte-interphase (SEI), respectively.^[19, 51] During the first delithiation process, one anodic peak located at ~0.7 can be ascribed to the phase transition of Li_xGe to Ge.^[19] The presence of another two cathodic peaks at 0.3 V and near 0.01 V after 1st cycle suggested that a number of different Li-Ge phases are formed during electrochemical lithiation.^[28, 51] The peaks become broader during lithium alloy process after the initial cycle, indicating that Ge nanoparticles converted to amorphous Ge. The difference between the first and the later cycles is partly ascribed to SEI formation and the local structure rearrangement in the electrode to accommodate the mechanical stress induced during alloying/dealloying.^[19, 37]

Fig. 3B displays the voltage profiles of Ge-CNFs electrode in the voltage window between 0.005 and 1.2 V (vs. Li⁺/Li) at a rate of 0.15 C. The voltage profiles indicate that the Ge-CNFs composite electrode exhibits the typical characteristics of Ge electrode. The initial discharge and charge capacities of Ge-CNFs electrode are 1278 and 883 mAh.g⁻¹, respectively, giving an initial Coulombic efficiency (CE) of ~70%. The large capacity loss of 1st cycle is mainly due to the formation of SEI layer on the electrode surface during the first discharge as the aforementioned reason and irreversible Li insertion into the CNFs matrix. The specific surface area of Ge-CNFs measured by the Brunauer-Emmett-Teller (BET) method is 299.15 m²g⁻¹ (see supporting information, Fig. S3). After the 1st cycle, the CE gradually increases and reaches ~100% after several cycles. Compare to commercial Ge powder shows a CE of about 16% (Fig. 3C), our Ge-CNFs electrode demonstrates noticeably improved

efficiency, which may be attributed to the carbon coating that minimized surface oxidation of Ge nanoparticles and protected Ge nanoparticles during cycling.^[12, 18]

The capacity retention of Ge-CNFs and commercial Ge powder are compared in **Fig. 3C**. The Ge-CNFs electrode shows a higher reversible specific capacity of over 800 mAhg⁻¹ in the first 10 cycles and maintains a reversible capacity of ~740 mAhg⁻¹ after 100 cycles at 0.15 C. To realize the electrochemical performance of Ge nanoparticles during cycling, the capacity contribution of Ge nanoparticles in the carbon matrix was calculated based on the weight of Ge.^[18, 52] The discharge capacity of the second cycle was 878 mAhg⁻¹ based on the electrode. Since carbon fibers can only provide a discharge capacity of 203 mAhg⁻¹ (see supporting information, Fig. S5B) at the same current density, the capacity contributed by Ge nanoparticles was ~1600 mAhg⁻¹, which corresponds to 97% of the theoretical capacity, demonstrating the full utilization of Ge nanoparticles.^[18] After 100 cycles at 0.15 C, the capacity contribution of Ge nanoparticles was ~1420 mAhg⁻¹, with only 0.1% decay per cycle. In case of the electrode made of commercial Ge powder, it only displays a discharge capacity (~300 mAhg⁻¹) for the first several cycles, then the capacity fade abruptly, due to the disconnection of material. The improved cycle performance of Ge-CNFs demonstrated that this special (Ge)_{0D}@(CNFs)_{1D} design could effectively buffer the volume change and keep electro-active material contact during the lithium incorporation/extraction.^[19]

The rate performance of Ge-CNFs was tested and the results were shown in Fig. 3D. The Ge-CNFs can deliver a reversible capacity of 1520, 1334, 1205, 1062, 769, 622, 475 and 272 mAhg⁻¹ based on the content of Ge at current densities of 0.35C, 0.8C, 1.5C, 3.5C, 8C, 12.5C, 15C and 25C, respectively.^[52] When the current density recover to 0.15C after 90 cycles, the specific capacity come back to 1496 mAh.g⁻¹, implying the good reversibility and stability of Ge-CNFs electrode.

To further get evidence of the improved performance of our Ge-CNFs electrode, we cycled the Ge-CNFs electrode at 1C for 250 cycles (Fig. 4). It still could deliver a superior capacity of 829 mAhg⁻¹ based on the content of Ge after 250 cycles. This excellent cycling stability of Ge-CNFs electrode could be possibly attributed to the

special structure. The nanoscaled Ge shorten the transport lengths for both electrons and lithium ions; the 3D interconnected CNFs framework be well preserved during cycling, which enhance the physical connection and electrical contact of Ge nanoparticles, thereby ensuring a reversible lithium alloying/dealloying process even at high current density. In addition, the Ge nanoparticles were fully encapsulated in CNFs not only prevents Ge from aggregation during charge/discharge but also keep the electrolyte from further decomposition while still providing the Li^+/e^- transport within Ge nanoparticles.

To confirm the structure stability of this Ge-CNFs electrode, we investigate the morphology of Ge-CNFs electrode after 100 cycles at a rate of 0.15C. As shown in Fig. 5, the continuous and interconnected structure of Ge-CNFs remained almost unchanged without any obvious pulverization and fracture of CNFs. Notably, the surface of Ge-CNFs electrode after cycles displays a rough surface that could be results from the formation of SEI and some residual electrolyte on the surface. This result indicates that the 3D interconnect CNFs network could mitigate the strains caused by the volume change during cycling and maintain the continuous and interconnected structure to provide short electron and ion transfer path upon long-term cycling(as illustrated in Fig. 6).

In summary, we present a unique 3D porous flexible Ge-CNFs nanostructure electrode consisting of Ge encapsulated in CNFs as a high-performance LIBs working electrodes using a simple, scalable, and low-cost electrospinning technique. The collected Ge-CNFs flexible films are directly applied as integrated self-supported and binder-free electrodes for LIBs. The Ge nanoparticles were well dispersed in the CNFs. The flexible Ge-CNFs electrode exhibits long-term stability upon cycling, good rate capability, and relatively high discharge capacity. The Ge-CNFs delivers a great specific reversible capacity of $\sim 1420 \text{ mAhg}^{-1}$ after 100 cycles at 0.15C, corresponding to 82% of the initial charge capacity. Even after 250 cycles at a high current of 1C, it still delivers a reversible specific capacity of 829 mAhg^{-1} . The improved electrochemical performance arises from synergistic effects of 0D Ge, 1D CNFs, and 3D interconnected CNFs framework, which could effectively

accommodate the huge volume change of Ge nanoparticles during cycling and maintain perfect electrical conductivity throughout the electrode. But when the whole electrode was considered to calculate the capacity, the performance of this kind of materials should be improved further, as the capacity of carbon matrix is not high. This problem might be solved through increasing the content of Ge or the capacity of the matrix in the future. However, this special electrode structure, encapsulation of nanoparticles in CNFs matrix prepared by electrospinning process provides a promising solution to design and synthesize other high-performance electrode materials for LIBs or other energy storage systems.

Experimental:

Preparation of precursor solutions of electrospinning: 0.4 g polyacrylonitrile (PAN, MW=150 000, Aldrich) and 1.5 g tetramethoxygermane (TMOG, Aldrich) were dissolved in 4.6 g *N,N*-dimethylformamide (DMF, Sinopharm Chemical Reagent Co., Ltd.) to prepare the electrospun nanofibers for Ge@CNFs.

Fabrication of polymer nanofibers via electrospinning: The above solution was loaded into two 10 mL syringe with a 19-gauge blunt tip needle respectively. Then these solutions were electrospun using an electrospinning system (UCALERY Beijing Co., LTD, China). The syringes were pushed by a syringe pump with a flow rate of 25.00 $\mu\text{L}\cdot\text{min}^{-1}$. An iron plate coated with an aluminum sheet, used as a polymer nanofibers collector, was placed 15 cm below the needle. Both the needle and the iron plate were connected to a high voltage power supply. Two high voltages of +15.00 kV and -1.00 kV were supplied at the spinneret and the iron plate respectively.

Preparation of Germanium-Carbon Nanofibers: The collected electrospun nanofibers were stabilized in air at 280 °C for 3h with a heating rate of 2 $\text{K}\cdot\text{min}^{-1}$. Subsequently, the above stabilized fibers were heated to 650 °C Ar/H₂ for 3h to obtain Ge-CNFs, where the heating rate was kept at 5 $\text{K}\cdot\text{min}^{-1}$.

Characterization: The structure of the obtained Ge-CNFs webs and precursors was characterized by X-ray diffraction (XRD) (TTR-III, Rigaku, Japan) using Cu K α radiation. Fourier transform infrared (FTIR) spectra were performed by a Thermo Nicolet 8700 FTIR spectrophotometer. Field-Emission Scanning electron microscopy (FESEM) investigations were performed using a JSM-6700 field-emission scanning electron microscope (JEOL, Tokyo, Japan) operated at 5keV. A JEOL 4000EX transmission electron microscope (HRTEM) (JEOL, Tokyo, Japan) was used to study the morphology and microstructure of Ge-CNFs. Nitrogen adsorption/desorption isotherms were measured with an ASAP 2020 Accelerated Surface Area and Porosimetry instrument.

Electrochemical Characterization: The freestanding Ge-CNFs (or CNFs) were directly used as the working electrodes (~1 mg, Diameter= ~14.5 mm, Thickness= ~0.5 mm) to perform batteries with 2032 coin cells with Li metal as counter and reference electrodes. Commercial Ge powder (purity \geq 99.999%, Sinopharm Chemical Reagent Co., Ltd.) electrodes were prepared by the common method, mixing commercial Ge powder, carbon black and poly(vinylidene fluoride) (PVDF) at a weight ration of 80:10:10 and pasted on pure Cu foil. The electrolyte was 1 M LiPF₆ in a mixture of EC and DEC (1:1 = w: w), and Celgard 2400 membrane was used as a separator. The cells were assembled in an argon-filled glovebox. The galvanostatic charge-discharge tests were conducted at a voltage interval of 0.005-1.2 V. Cyclic voltammetry measurements were conducted at a scan rate of 0.2 mVs⁻¹ on a CHI 660D electrochemical workstation (Chenhua Instrument Company, Shanghai, China).

Acknowledgements

This work was financially supported by the National Natural Science Foundation of China (No.21171015 and No. 21373195), the “1000 plan” from Chinese Government, program for New Century Excellent Talents in University (NCET-12-0515), the Fundamental Research Funds for the Central Universities (WK2060140014) and sofja kovalevskaja award from Alexander von Humboldt Foundation.

Reference:

- [1] B. Scrosati, *Nature* 1995, 373, 557.
- [2] P. G. Bruce, B. Scrosati, J. M. Tarascon, *Angewandte Chemie - International Edition* 2008, 47, 2930.
- [3] P. Poizot, S. Laruelle, S. Grugeon, L. Dupont, J. M. Tarascon, *Nature* 2000, 407, 496.
- [4] V. Etacheri, R. Marom, R. Elazari, G. Salitra, D. Aurbach, *Energy and Environmental Science* 2011, 4, 3243.
- [5] M. Thackeray, *Nature Materials* 2002, 1, 81.
- [6] J. M. Tarascon, M. Armand, *Nature* 2001, 414, 359.
- [7] K. Evanoff, A. Magasinski, J. Yang, G. Yushin, *Advanced Energy Materials* 2011, 1, 495.
- [8] G. Cui, L. Gu, N. Kaskhedikar, P. A. van Aken, J. Maier, *Electrochimica Acta* 2010, 55, 985.
- [9] Y. Yu, L. Gu, X. Lang, C. Zhu, T. Fujita, M. Chen, J. Maier, *Advanced Materials* 2011, 23, 2443.
- [10] Y. Yu, L. Gu, C. Zhu, S. Tsukimoto, P. A. Van Aken, J. Maier, *Advanced Materials* 2010, 22, 2247.
- [11] C. K. Chan, X. F. Zhang, Y. Cui, *Nano Letters* 2008, 8, 307.
- [12] M. H. Park, Y. Cho, K. Kim, J. Kim, M. Liu, J. Cho, *Angewandte Chemie - International Edition* 2011, 50, 9647.
- [13] H. Kim, Y. Son, C. Park, J. Cho, H. C. Choi, *Angewandte Chemie - International Edition* 2013, 52, 5997.
- [14] D. J. Xue, S. Xin, Y. Yan, K. C. Jiang, Y. X. Yin, Y. G. Guo, L. J. Wan, *Journal of the American Chemical Society* 2012, 134, 2512.
- [15] M. H. Park, K. Kim, J. Kim, J. Cho, *Advanced Materials* 2010, 22, 415.
- [16] F. W. Yuan, H. J. Yang, H. Y. Tuan, *ACS Nano* 2012, 6, 9932.
- [17] Y. Yu, C. Yan, L. Gu, X. Lang, K. Tang, L. Zhang, Y. Hou, Z. Wang, M. W. Chen, O. G. Schmidt, J. Maier, *Advanced Energy Materials* 2013, 3, 281.
- [18] C. Wang, J. Ju, Y. Yang, Y. Tang, J. Lin, Z. Shi, R. P. S. Han, F. Huang, *Journal of Materials Chemistry A* 2013, 1, 8897.
- [19] M. H. Seo, M. Park, K. T. Lee, K. Kim, J. Kim, J. Cho, *Energy and Environmental Science* 2011, 4, 425.
- [20] K. H. Seng, M. H. Park, Z. P. Guo, H. K. Liu, J. Cho, *Angewandte Chemie - International Edition* 2012, 51, 5657.
- [21] W. Liang, H. Yang, F. Fan, Y. Liu, X. H. Liu, J. Y. Huang, T. Zhu, S. Zhang, *ACS Nano* 2013, 7, 3427.
- [22] I. S. Hwang, J. C. Kim, S. D. Seo, S. Lee, J. H. Lee, D. W. Kim, *Chemical Communications* 2012, 48, 7061.
- [23] X. H. Liu, S. Huang, S. T. Picraux, J. Li, T. Zhu, J. Y. Huang, *Nano Letters* 2011, 11, 3991.
- [24] L. C. Yang, Q. S. Gao, L. Li, Y. Tang, Y. P. Wu, *Electrochemistry Communications* 2010, 12, 418.

- [25]N. G. Rudawski, B. L. Darby, B. R. Yates, K. S. Jones, R. G. Elliman, A. A. Volinsky, *Applied Physics Letters* 2012, 100.
- [26]T. Song, Y. Jeon, M. Samal, H. Han, H. Park, J. Ha, D. K. Yi, J. M. Choi, H. Chang, Y. M. Choi, U. Paik, *Energy and Environmental Science* 2012, 5, 9028.
- [27]Y. D. Ko, J. G. Kang, G. H. Lee, J. G. Park, K. S. Park, Y. H. Jin, D. W. Kim, *Nanoscale* 2011, 3, 3371.
- [28]L. P. Tan, Z. Lu, H. T. Tan, J. Zhu, X. Rui, Q. Yan, H. H. Hng, *Journal of Power Sources* 2012, 206, 253.
- [29]Y. J. Cho, C. H. Kim, H. S. Im, Y. Myung, H. S. Kim, S. H. Back, Y. R. Lim, C. S. Jung, D. M. Jang, J. Park, S. H. Lim, E. H. Cha, K. Y. Bae, M. S. Song, W. I. Cho, *Physical Chemistry Chemical Physics* 2013, 15, 11691.
- [30]J. G. Ren, Q. H. Wu, H. Tang, G. Hong, W. Zhang, S. T. Lee, *Journal of Materials Chemistry A* 2013, 1, 1821.
- [31]H. Lee, H. Kim, S. G. Doo, J. Cho, *Journal of the Electrochemical Society* 2007, 154, A343.
- [32]G. Cui, L. Gu, L. Zhi, N. Kaskhedikar, P. A. Van Aken, K. Müllen, J. Maier, *Advanced Materials* 2008, 20, 3079.
- [33]H. Lee, J. Cho, *Nano Letters* 2007, 7, 2638.
- [34]C. K. Chan, H. Peng, G. Liu, K. McIlwrath, X. F. Zhang, R. A. Huggins, Y. Cui, *Nat Nano* 2008, 3, 31.
- [35]M. S. Park, G. X. Wang, Y. M. Kang, D. Wexler, S. X. Dou, H. K. Liu, *Angewandte Chemie - International Edition* 2007, 46, 750.
- [36]S. Mathur, H. Shen, N. Donia, T. Rügamer, V. Sivakov, U. Werner, *Journal of the American Chemical Society* 2007, 129, 9746.
- [37]Y. Yu, L. Gu, C. Wang, A. Dhanabalan, P. A. Van Aken, J. Maier, *Angewandte Chemie - International Edition* 2009, 48, 6485.
- [38]T. H. Hwang, Y. M. Lee, B. S. Kong, J. S. Seo, J. W. Choi, *Nano Letters* 2012, 12, 802.
- [39]Y. Yu, L. Gu, C. Zhu, P. A. Van Aken, J. Maier, *Journal of the American Chemical Society* 2009, 131, 15984.
- [40]F. Xia, S. B. Kim, H. Cheng, J. M. Lee, T. Song, Y. Huang, J. A. Rogers, U. Paik, W. I. Park, *Nano Letters* 2013, 13, 3340.
- [41]G. Jo, I. Choi, H. Ahn, M. J. Park, *Chemical Communications* 2012, 48, 3987.
- [42]R. A. Dileo, S. Frisco, M. J. Ganter, R. E. Rogers, R. P. Raffaele, B. J. Landi, *Journal of Physical Chemistry C* 2011, 115, 22609.
- [43]M. Inagaki, Y. Yang, F. Kang, *Advanced Materials* 2012, 24, 2547.
- [44]S. Cavaliere, S. Subianto, I. Savych, D. J. Jones, J. Rozière, *Energy and Environmental Science* 2011, 4, 4761.
- [45]H. Miguez, F. Meseguer, C. Lopez, M. Holgado, G. Andreasen, A. Mifsud, V. Fornes, *Langmuir* 2000, 16, 4405.
- [46]R. R. Moskalyk, *Minerals Engineering* 2004, 17, 393.
- [47]Z. Yang, J. G. C. Veinot, *Journal of Materials Chemistry* 2011, 21, 16505.
- [48]C. Zhu, Y. Yu, L. Gu, K. Weichert, J. Maier, *Angewandte Chemie - International Edition* 2011, 50, 6278.

- [49]S. W. Choi, J. R. Kim, S. M. Jo, W. S. Lee, Y. R. Kim, Journal of the Electrochemical Society 2005, 152, A989.
- [50]L. G. Bulusheva, A. V. Okotrub, A. G. Kurennya, H. Zhang, H. Zhang, X. Chen, H. Song, Carbon 2011, 49, 4013.
- [51]J. Wang, N. Du, H. Zhang, J. Yu, D. Yang, Journal of Materials Chemistry 2012, 22, 1511.
- [52]Y. Zhu, X. Han, Y. Xu, Y. Liu, S. Zheng, K. Xu, L. Hu, C. Wang, ACS Nano 2013, 7, 6378.

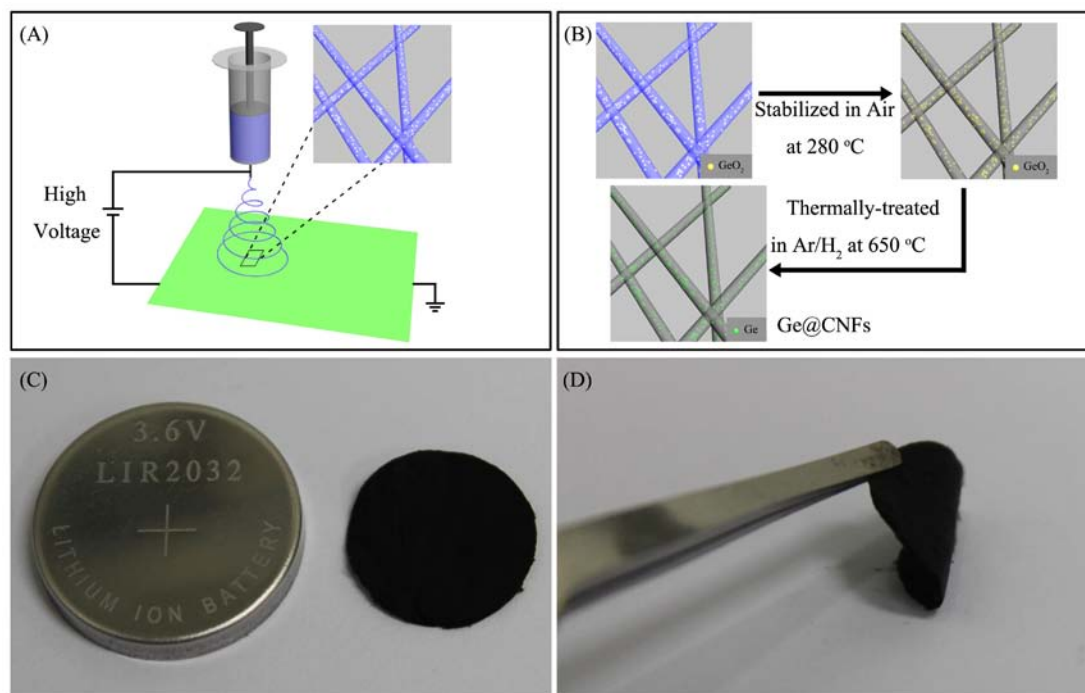


Fig. 1 A~B Schematic illustration of the synthesis process for the Ge@CNFs electrode.

Fig. 1 C~D Photograph of free-standing and flexible Ge@CNFs electrode.

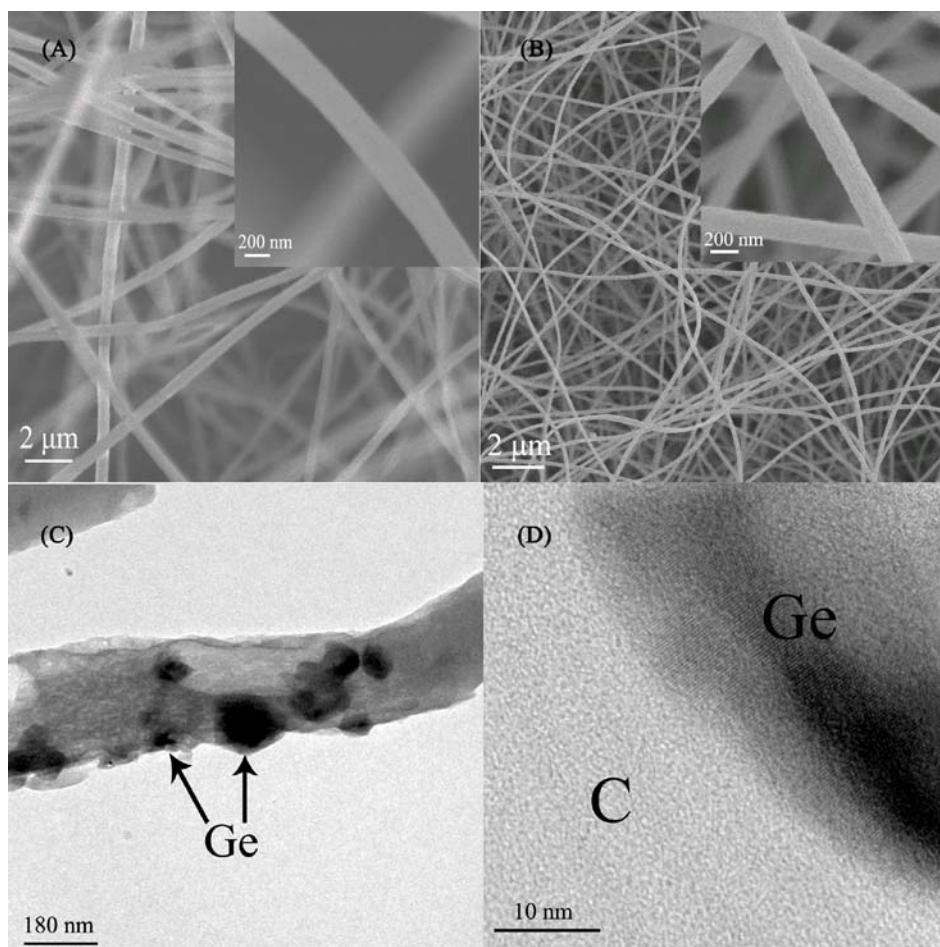


Fig. 2 FESEM micrographs of as-electrospun PAN-TMOG nanofibers (A) and Ge@CNFs nanofibers (B). The inset pictures are corresponding high magnification images. TEM (C) and HRTEM (D) micrographs of Ge-CNFs.

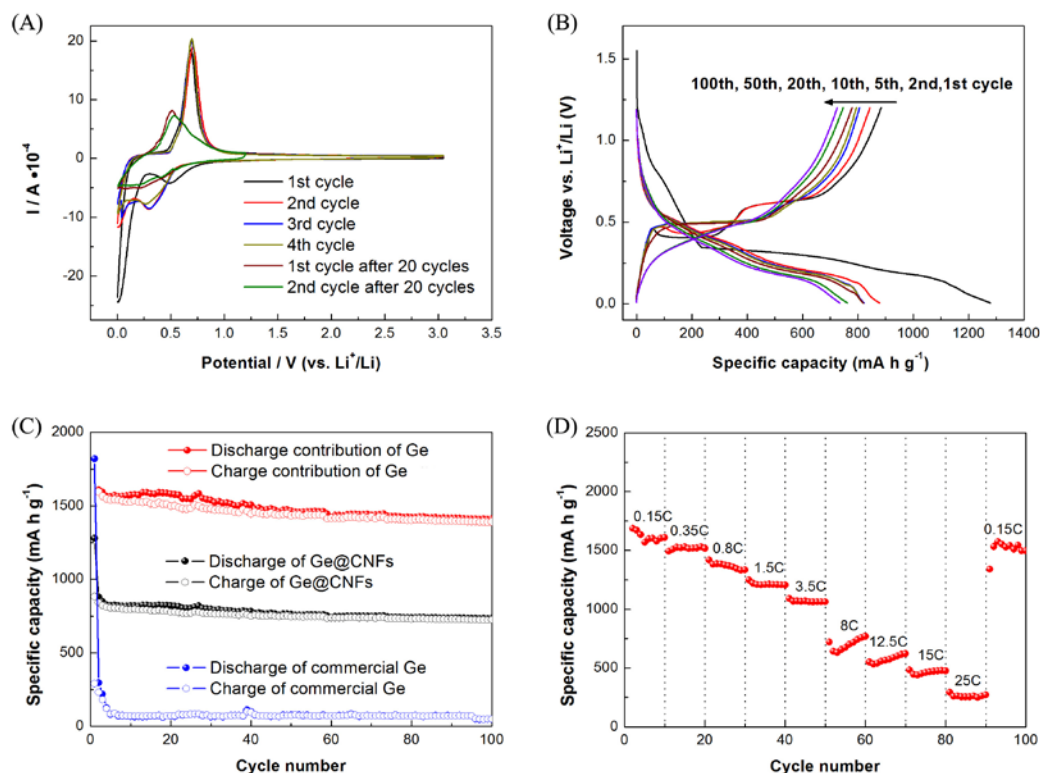


Fig. 3 (A): Cyclic voltammograms of Ge-CNFs at a scan rate of 2 mVs^{-1} (voltage range: 5mV–1.2 V). (B): Voltage profiles of Ge-CNFs electrodes cycled between 0.005V and 1.2 V vs. Li^+/Li at a cycling rate of 0.15C ($243 \text{ mA/g}_{\text{Ge}}$). (C)&(D): Electrochemical performance of Ge-CNFs and commercial Ge powder electrode cycled between 0.005 V and 1.2 V vs. Li^+/Li . (C): Capacity-cycle number curves of Ge-CNFs and commercial Ge powder electrodes at a cycling rate of 0.15 C; (D): Discharge capacity of Ge-CNFs electrodes as a function of discharge rate (0.15C ~ 25C).

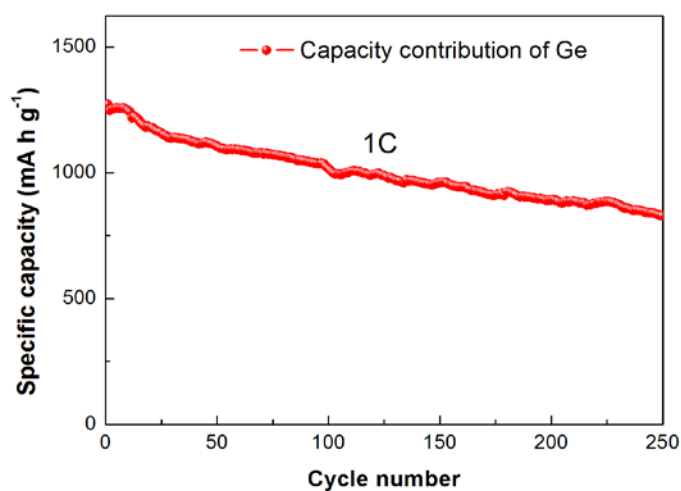


Fig. 4 Cycle performance of Ge@CNFs electrodes at 1C (1624 mA/g_{Ge}) for 250 cycles. (The batteries were activated firstly at a cycling rate of 0.15C for ten times).

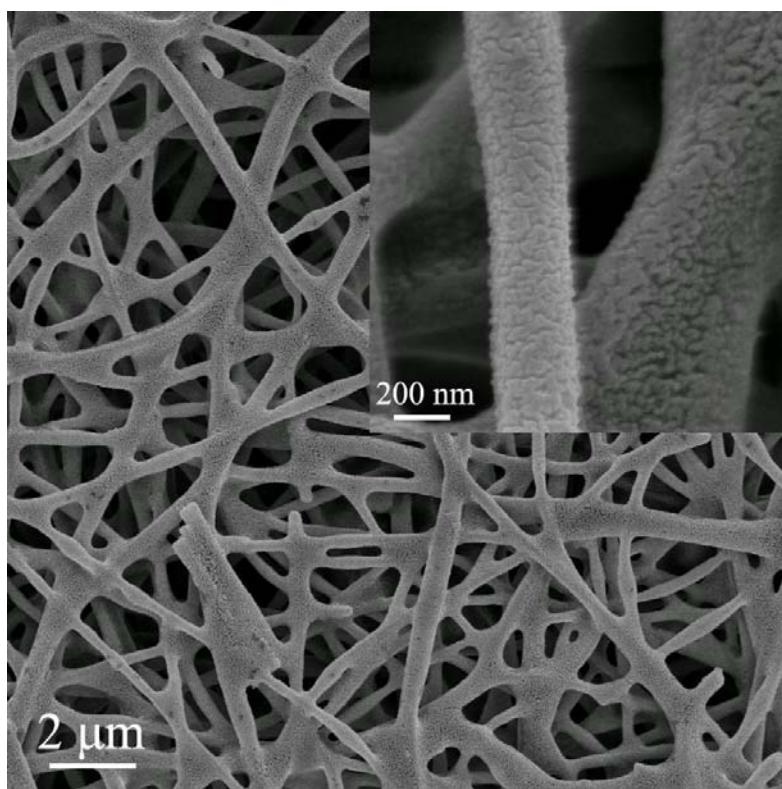


Fig. 5 FESEM micrographs of Ge@CNFs after 100 cycles between 0.005V and 1.2 V vs. Li⁺/Li at a cycling rate of 0.15C, inset shows the corresponding high magnification image.

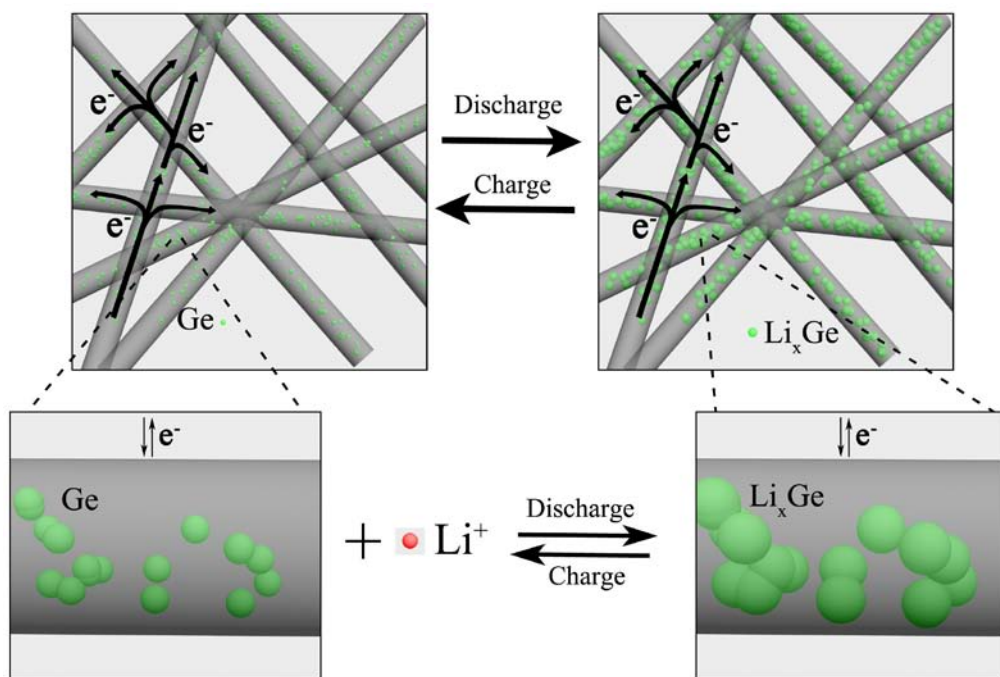


Fig. 6 Schematic illustration of the alloying/de-alloying reaction mechanism of Ge@CNFs during cycling.

Supporting Information

Germanium Nanoparticles Encapsulated in Flexible Carbon Nanofibers as Self-Supported Electrodes for High performance Lithium-ion Batteries

Weihan Li, Zhenzhong Yang, Jianxiu Cheng, Xiongwu Zhong, Lin Gu, Yan Yu[†]

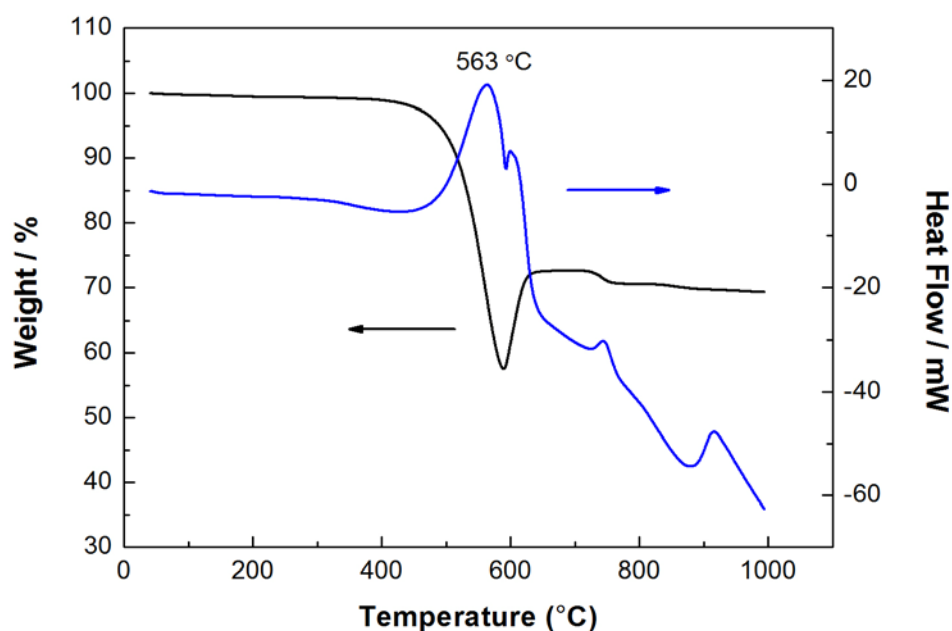


Fig. S1 Thermogravimetric analysis (TGA) and Differential scanning calorimetry (DSC) of the Ge-CNFs. The content of Ge in the Ge-CNFs estimated from the TGA is ca. 48.1 wt%. (Note: Ge was totally oxidized into GeO_2). This analysis was taken in air with a heating rate of $10\text{ }^\circ\text{C min}^{-1}$.^[1]

W. Li, J. Cheng, X. Zhong, Prof. Y. Yu
CAS Key Laboratory of Materials for Energy Conversion, Department of Materials Science and Engineering,
University of Science and Technology of China, Anhui Hefei 230026, P. R. China
E-mail: yanyumse@ustc.edu.cn
Z. Yang, Prof. L. Gu
Beijing National Laboratory for Condensed Matter Physics, The Institute of Physics, Chinese Academy of
Sciences, Beijing 100190, P. R. China

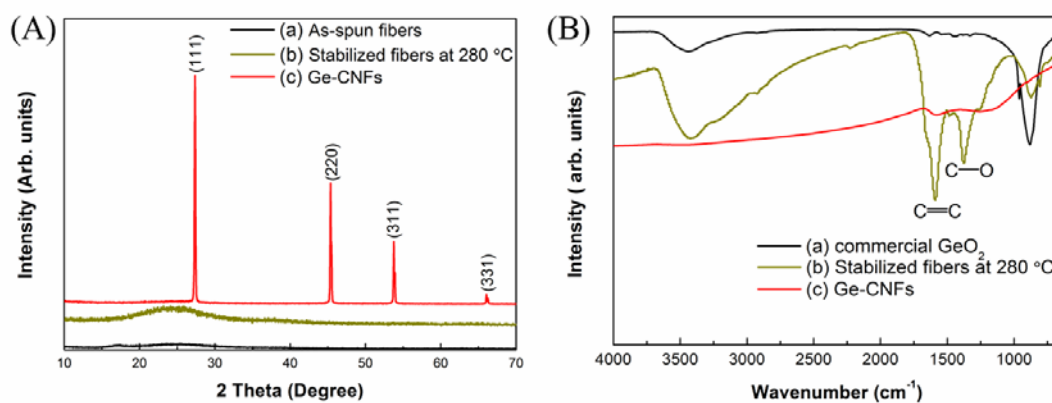


Fig. S2 (A) XRD patterns of as-spun fibers (a), stabilized fibers (b) and Ge-CNFs (c). (B) Fourier transform infrared (FTIR) spectroscopy of commercial GeO₂ (a), stabilized fibers (b) and Ge-CNFs (c).

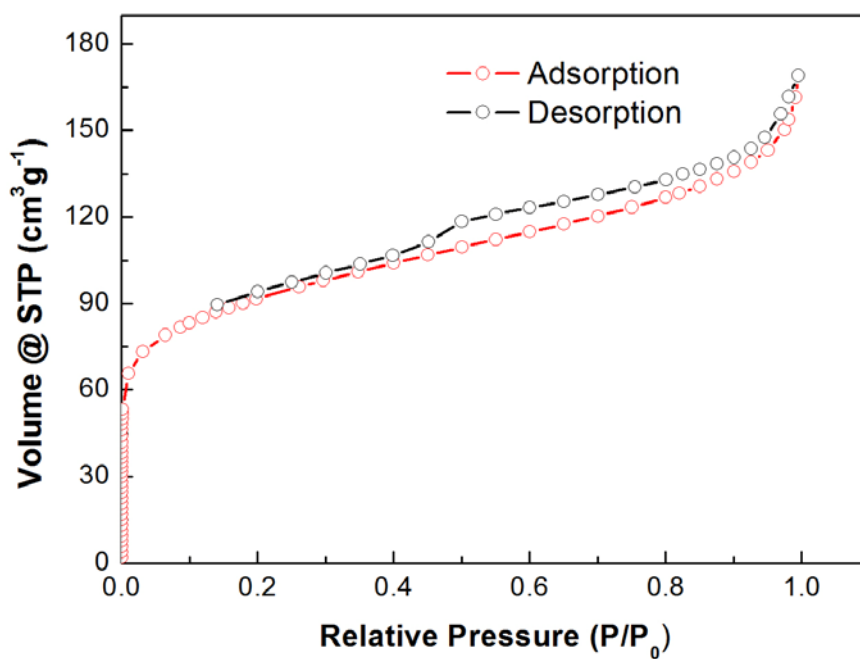


Fig. S3 N₂ sorption/desorption isotherm of Ge-CNFs. The Brunauer-Emmett-Teller (BET) specific surface of the P-CNFs investigated here as 299.15 m²g⁻¹.

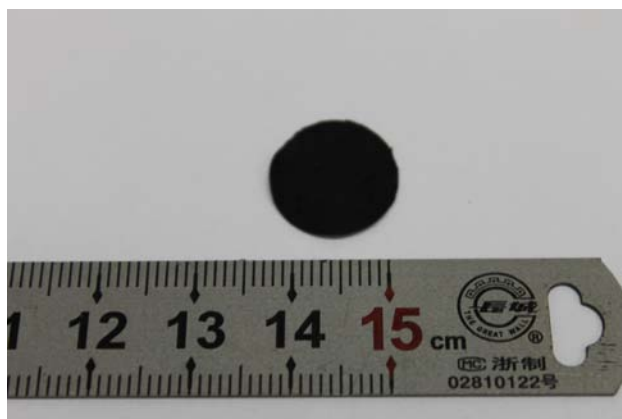


Fig. S4 Photograph of free-standing and flexible carbon nanofibers electrode.

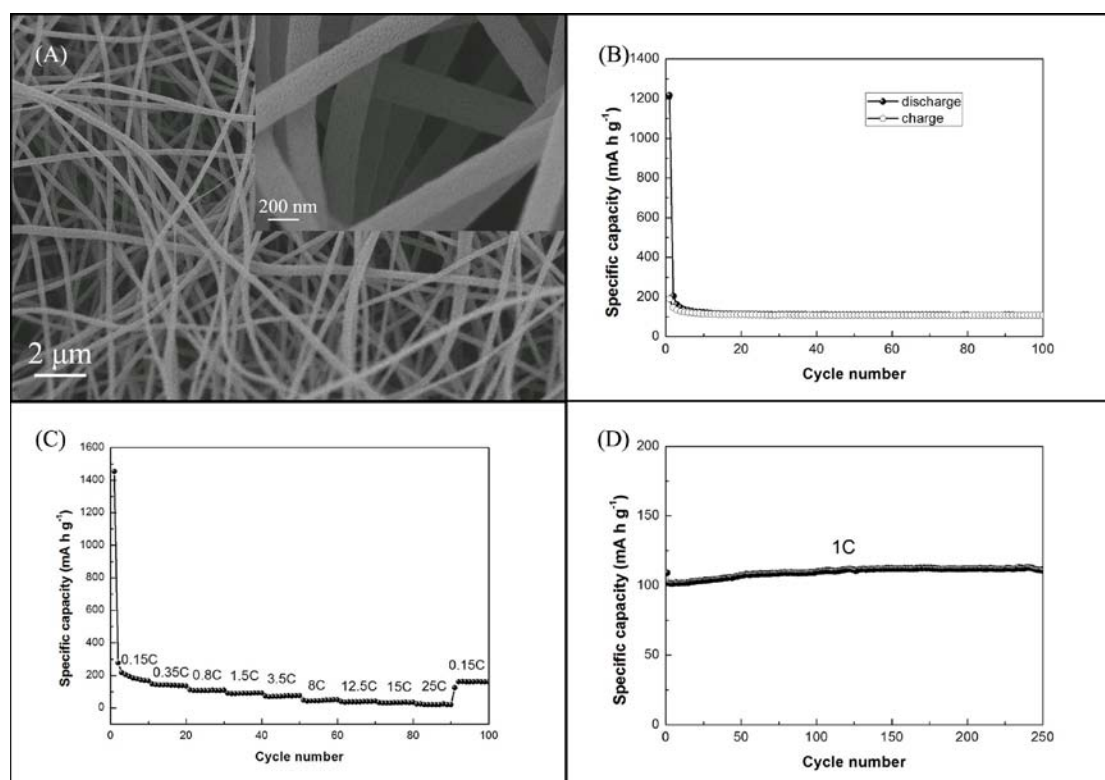


Fig. S5 (A) FESEM micrographs of electrospun carbon fibers generated from pure PAN. Electrochemical performance of carbon nanofibers cycled between 0.005 V and 1.2 V vs. Li^+/Li . (B): Capacity-cycle number curves of carbon nanofibers at a cycling rate of 0.15 C; (C): Discharge capacity of carbon nanofibers electrodes as a function of discharge rate (0.15C ~ 25C); (D): Capacity-cycle number curves of carbon nanofibers at a cycling rate of 1 C;

[1] J. G. Ren, Q. H. Wu, H. Tang, G. Hong, W. Zhang, S. T. Lee, *Journal of Materials Chemistry A* 2013, 1, 1821.